

DESIGN AND TESTING OF NEW SMOKE CONCENTRATION METER

by

**George W. Mulholland, Erik L. Johnsson
and Marco G. Fernandez
Building and Fire Research Laboratory
National Institute of Standards and Technology
Gaithersburg, MD 20899 USA
and
David A. Shear
Massachusetts Institute of Technology
Cambridge, MA 02139, USA**

Reprinted from the Fire and Materials, Vol. 24, No. 5, 231-243, September/October 2000.

NOTE: This paper is a contribution of the National Institute of Standards and Technology and is not subject to copyright.



NIST

National Institute of Standards and Technology
Technology Administration, U.S. Department of Commerce

Design and Testing of a New Smoke Concentration Meter

George W. Mulholland^{1*}, Erik L. Johnsson¹, Marco G. Fernandez¹ and David A. Shear²

¹National Institute of Standards and Technology, Gaithersburg, MD 20899, USA

²Massachusetts Institute of Technology, Cambridge, MA 02139, USA

The design of a new smoke concentration meter based on light-extinction measurements with a He-Ne laser is described. The measurement allows the determination of the mass-generation rate of smoke and smoke yield during a fire test with little more time or labour than is required for performing heat-release-rate and mass-loss-rate measurements. The new smoke concentration meter was motivated by the finding from several studies of a nearly universal value of the specific extinction coefficient of post-flame smoke produced by over ventilated fires. Key design features include the use of a stabilized laser, purge flow to eliminate smoke deposition on the optics, U channel construction to minimize the effect of heating on the optical alignment and beam correction optics. The facility was fabricated almost entirely from commercially available components to allow this design to be easily reproduced by fire research and testing laboratories. The smoke concentration meter was able to measure a smoke yield as small as 0.005 for a propane fire to as large as 0.10 for a toluene pool fire. A detailed uncertainty assessment was made. The result for a 50 cm diameter heptane pool fire agrees well with previous smoke yield measurements made for the same fuel and pool diameter based on filter collection and weighing. Copyright © 2000 John Wiley & Sons Ltd.

INTRODUCTION

An important parameter in assessing the fire safety of a new product is the smokiness of the material as it affects visibility and fire spread. Materials with a tendency to produce high levels of smoke make it more difficult for people to egress from the affected area. Minimizing smoke is especially important in transportation systems such as airplanes, trains and subways. The smoke particulate in a flame is a major contributor to the flame radiation, which is a major mechanism for flame spread in developing fires.

Smoke also has a large economic impact as it deposits on surfaces. Two of the most costly impacts result from smoke deposition in communication systems and computer facilities. Smoke deposition is also a major concern in high cost production facilities where a clean environment is crucial such as for semiconductor fabrication and for pharmaceutical preparation.

One measure of the smokiness of a material is its smoke yield, ε , which is defined as the mass of smoke aerosol (particulate or droplets) produced per mass of material burned. This quantity ranges from 0.005 for the flaming combustion of wood cribs to as high as 0.15 for polystyrene.¹ The rate of smoke production during a fire depends on both the value of ε and on the mass loss rate of the fuel, \dot{m} . So it is possible for a material with a large ε , but small \dot{m} , to produce less total smoke than a material with a higher burning rate and an average \dot{m} . Thus smoke yield and burning rate of a material are both important.

One method of measuring smoke production is to use a sampling probe to collect a fraction of the total flow through an exhaust stack on a filter. This method has been used at National Institute of Standard and Techno-

logy (NIST) at both small scale with the cone calorimeter and at large scale with the furniture calorimeter.² Filter collection has also been used at a number of other facilities including Factory Mutual Research Corporation,³ Georgia Tech Combustion Characterization Facility,⁴ and the University of Michigan Buoyant Turbulent Flame Facility.⁵ This method has the advantage that it provides a direct gravimetric measurement of the total mass of smoke produced over the collection period. Difficulties with filter collection include limited time resolution and particle deposition in sampling tubes as a result of thermophoresis. However, the major difficulty is the large labour cost for processing filter samples, which must be treated with care to obtain accurate results. This high cost has limited the use of the filter collection method for evaluating the smokiness of a material.

The cone calorimeter has been widely used to measure the specific-extinction area⁶ of a burning material σ_f , which is the light-extinction coefficient, K , normalized by the mass loss rate of the sample, \dot{m}_f , per volume flow rate, \dot{V} , through the collection hood.

$$\sigma_f = \frac{K}{\dot{m}_f/\dot{V}} \quad (1)$$

The quantity K is defined in terms of the intensity ratio of the incident and transmitted light, I_o/I , and the path-length through the smoke, L , by the equation

$$K = \frac{\ln(I_o/I)}{L} \quad (2)$$

The quantity σ_f is a useful measure for the relative smokiness of materials with values ranging from as small as 0.03 m²/g for a wood 'crib' to as large as 1.0 m²/g for crude oil. However, the most basic property of the smoke

*Correspondence to: Dr. G. W. Mulholland, National Institute of Standards and Technology, Gaithersburg, MD 20899, USA.

aerosol is its mass concentration M_s . To compute the mass concentration of the smoke in a room resulting from a fire, one needs to know the mass generation rate of the smoke or the yield of smoke. Given the mass concentration one can make first order estimates of smoke detector response, visibility through the smoke, amount of smoke deposited on the ceiling and the floor, and thermal radiation reaching the floor if the upper layer temperature is known. More quantitative estimates of these effects would also require information on the number concentration of the smoke, the optical properties of the smoke, and the smoke particle size distribution.

This paper establishes a methodology for determining the mass concentration of flame-generated smoke by performing a light-extinction measurement such as made in the cone calorimeter and the furniture calorimeter.² Bouguer's Law relates the ratio of the transmitted and incident intensities to the mass concentration of smoke M_s , the pathlength through the smoke, L , and the specific extinction coefficient σ_s via the following expression

$$\frac{I}{I_o} = \exp(-\sigma_s M_s L) \quad (3)$$

The ability to infer mass concentration from a light extinction measurement is made possible by the discovery that σ_s is nearly universal for post-flame smoke produced from overventilated fires. In a companion paper to this, Mulholland and Croarkin⁷ report that σ_s has an average value of $8.7 \text{ m}^2/\text{g}$ at a wavelength of 632.8 nm with an uncertainty interval of $\pm 1.1 \text{ m}^2/\text{g}$ at a 95% confidence level. The analysis in that paper⁷ is based on seven studies at five laboratories involving small and large-scale flames and a wide variety of fuel chemistries representative of combustible materials found in buildings. The basic qualitative ideas that support this universality are that soot from all flames is basically carbon in the form of agglomerates with primary sphere sizes much smaller than the wavelength of light and a fractal dimension less than two.⁸ For these conditions the light absorption cross section is proportional to the mass and is the dominant contribution to the light-extinction coefficient. There will be a smaller contribution from the light scattering cross section which depends on the agglomerate size.

The major focus of this paper is on the design of a new smoke concentration meter that takes advantage of this universal property of smoke to provide a direct reading of the mass concentration of the smoke. In the section entitled 'Design of the Smoke Concentration Meter' the features of the instrument will be described in relation to design requirements established by Putorti.⁹ One key feature of the design is to use commercially available components so this instrument can be duplicated by other fire laboratories.

The new smoke concentration meter was installed on a real-scale fire-testing apparatus at NIST.¹⁰ The results of a series of tests are described and the methodology for assessing the instrument uncertainty is presented. A series of tests was performed with heptane to compare with previous measurements of the smoke yield² for an 0.5 m pool fire. Also a test was carried out using toluene to assess the smoke concentration meter performance

near the maximum level expected for fire sizes up to 500 kW .

DESIGN REQUIREMENTS FOR A STACK MOUNTED LIGHT-EXTINCTION MEASUREMENT DEVICE

Putorti⁹ has developed requirements/characteristics for smoke meters based on experiences at NIST and a review of the literature. He reports that the following systems are accepted by standards organizations for light transmission measurements: ASTM E 84-91 'Standard Test Method for Surface Burning Characteristics of Building Materials',¹¹ ASTM E 662-93 'Standard Test Method for Specific Optical Density of Smoke Generated by Solid Materials',¹² ASTM E 906-83 'Standard Test Method for Heat and Visible Smoke Release for Materials and Products',¹³ ASTM E 1354-92 'Standard Test Method for Heat and Visible Smoke Release Rates for Materials and Products Using an Oxygen Consumption Calorimeter',¹⁴ and UL 217 'Single and Multiple Station Smoke Alarms'.¹⁵ Only the ASTM E 1354-92 smoke meter employs a monochromatic light source, which is necessary for satisfying Bouguer's law given in Eqn (3).

There are a number of commercially available devices for monitoring the opacity of effluents from industrial discharges. The technology is sophisticated, requiring 24-h-a-day operation, minimal maintenance and self-calibration. A number of innovations have been used including a double-pass design with a retro-reflector, pulsed light sources with phase-sensitive detection, and the use of a filter wheel for calibration.¹⁶ These devices are designed to meet US Environmental Protection Agency (EPA) requirements^{17,18} in terms of the allowable opacity, which corresponds to a light transmission of about 80%. Opacity meters are optimized for readings near the EPA Stack Emission value, and these devices are not suitable for measuring the much higher opacities commonly encountered in fire tests.

The report by Putorti⁹ contains instrument performance requirements for installation of a smoke concentration meter in the NIST Furniture Calorimeter,¹⁰ which has a duct with a diameter of 0.485 m , a nominal volumetric flow rate of $2 \text{ m}^3/\text{s}$, and can be used for fires ranging in size from about 50 kW to 500 kW . The first requirement is that, with no smoke present, the laser intensity shall drift by no more than $\pm 0.0024\%$ of I_{avg} over a 20 min period ($0.9976I_{\text{avg}} < I < 1.0024I_{\text{avg}}$), where I_{avg} is the 20 min average of the intensity. This requirement is needed for accurate measurements of materials generating low amounts of smoke such as expected for flaming combustion of a wood crib with a heat release rate of about 50 kW .

The second requirement concerns the instrument's performance when the transmitted light intensity is reduced to 2.5% of the incident intensity. This reduction in light intensity approximately corresponds to the burning of polystyrene at a heat release rate of 400 kW .⁹ For a neutral density filter set to transmit 2.5% of the incident light, the smoke concentration meter response should be within the range 2.26% to 2.74%. The light-extinction coefficient corresponding to 2.5% transmission for

a 0.485 m pathlength is 7.61 and the range in transmission values given above corresponds to a relative range in the extinction coefficient of about $\pm 3\%$.

Other recommended design characteristics include a small acceptance angle of the detector to minimize forward-scattered light, purge air to prevent soot deposition, resistance to vibrations in the duct, ease of alignment and calibration and a cost not to exceed about \$10 000. In the next section, the design of a system will be described which meets the requirements given above.

DESIGN OF SMOKE CONCENTRATION METER

We have developed a light-extinction meter based on the design guidelines given above. The major components are a He-Ne laser with a laser stabilizer, a silicon photodiode detector and associated optics to minimize the effect of beam movement, purge tubes to prevent smoke deposition on the windows and to minimize forward scattered light from reaching the detector, and both lateral and rotational positioning equipment for ease in alignment of the laser beam and the detector. These

components were obtained from commercial sources and the items and sources are listed in Table 1. The one major component fabricated at NIST was the structural support for mounting the smoke concentration meter. Our discussion below begins with the mounting of the meter and then describes the design features of the smoke concentration meter components.

The smoke concentration meter has been incorporated into the NIST furniture calorimeter.¹⁰ An overall schematic of the furniture calorimeter including the smoke concentration meter is illustrated in Fig. 1. The smoke flow makes a 90° bend just above the collection hood then continues downstream to the smoke concentration meter. A flow straightener¹⁹ just after the bend divides the flow up into 24 sections by use of three axial partitions and eight radial partitions with one every 45°. The smoke concentration meter assembly was mounted on a 61 cm (2 ft) long, 4.8 mm (3/16 in) thick section of steel duct with flanges on each end. This flanged tubing/meter was inserted in the duct by moving the wheel mounted hood assembly. The nominal Reynolds number for flow through the duct was 4×10^5 ensuring that the flow was turbulent. The smoke concentration meter was located about seven tube diameters downstream of the flow-straightening vanes.

Table 1. Smoke concentration meter components^a

Assembly	Component	Vendor/part number
Light source assembly	2.0 mW HeNe laser	Melles Griot, O5LHP121
	Laser power supply	Melles Griot, O5LPL 911-065
	Laser stabilizer	Thor Labs, CR200-A
	Adjustable holder for laser	Melles Griot, 07HLA015
	Standard translator with 1" travel	Oriel, 16161
	Mounting plate	Melles Griot, 07RPC025
	Dual stable rod with lead screw and horizontal mounting plate	Melles Griot, 07DPP015
Detector assembly	Housing for detector/optics ^b	Reyer Corp., SDA-100, (11847-B Lime Plant Rd., New Market, MD 21774)
	Si photodiode 1 cm diameter with quartz window	Hamamatsu Corp., S1227-1010
	Operation amplifier	BQ
	2-1 in diameter stackable lens tube (length 1 in and 2 in)	Burr Brown, OPA-627 BM
	6 retaining rings	Thorlabs, SM1 L05
	Spanner wrench for rings	Thorlabs, SMIRR
	Precision laser positioning system	Thorlabs, SPW 602
	Precision plano-convex lens with 50 mm focal length and HEBAR coating	Melles Griot, 07HLA535
		Melles Griot, 01LLP 013078
	Peripheral components	20 L/min air pump
BK7 window, 25 mm diameter, 3 mm thick with antireflection coating for purge tube		Melles Griot, 02WBK003/078

^a Certain commercial equipment, instruments, or materials are identified in this paper to specify adequately the experimental procedure. Such identification does not imply recommendation or endorsement by the National Institute of Standards and Technology of the specific equipment nor does it imply that the equipment listed is the best available.

^b Includes power supply for detector, 10 k Ω Caddock low temperature coefficient resistor, 10 μ F capacitor, circuit board with connector for the detector, optical mounting assembly for both focusing the beam with a 50 mm focal length lens and diffusing the beam as it reaches the detector. The optical mounting also includes a support for a neutral density filter. The design is modular so that the electronics assembly can be removed during the alignment process.

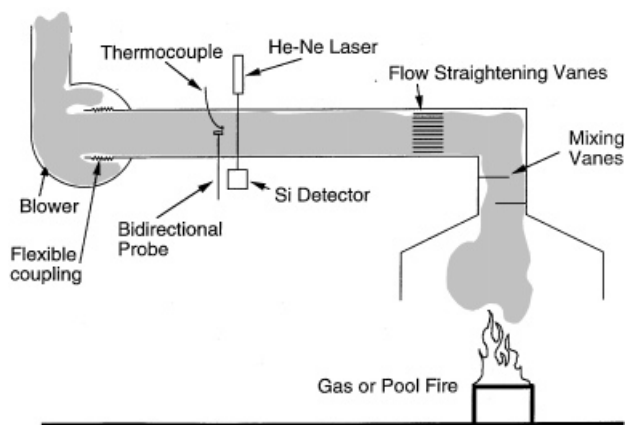


Figure 1. Overall schematic of furniture calorimeter with stack diameter 0.485 m and the smoke concentration meter positioned seven tube diameters downstream from the flow straightening vanes.

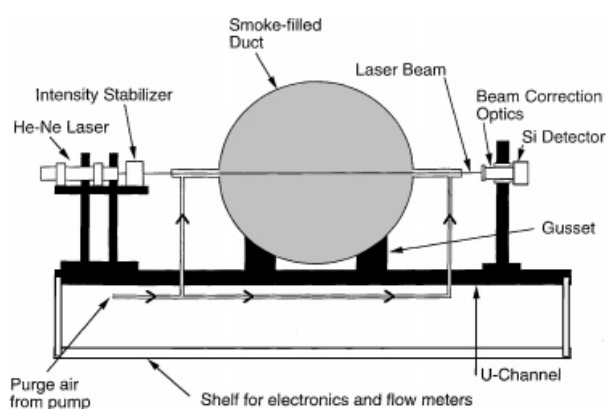


Figure 2. Overall schematic of smoke concentration meter.

One design requirement was that the system not be affected by vibrations in the duct caused by the exhaust blower. The furniture calorimeter minimized vibrations by including a flexible section of tubing between the steel duct and the blower. The effect of the thermal expansion of the duct was a more challenging design issue not specifically addressed in the report by Putorti. A 200°C increase in temperature would increase the circumference of the pipe by about 3.4 mm and the diameter by about 1 mm. This expansion can lead to both vertical and angular displacement of the detector versus the laser beam. To minimize this effect, both the light source assembly and the detector assembly were attached to a rigid U-channel made of steel [15.2 cm (6 in) wide with 0.79 cm (5/16 in) web], which was, in turn, attached to the duct with gussets welded to the duct as indicated in Fig. 2.

To prevent smoke deposition on the windows, two 2.5 cm diameter steel pipes were welded to the 48.5 cm diameter duct. The pipes were aligned so that the laser beam travelled along the centreline of both pipes as indicated in Fig. 2. The windows at the end of the tubes were coated to minimize reflections; in addition, the tube had been cut 3° from perpendicular to prevent interference between the transmitted beam and multiple reflec-

ted beams. The airflow through the tube was adjusted so that during a test the smoke neither penetrated into the tube or was 'blown' away from the tube entrance. A transparent purge tube was assembled for making the observation and the best flow rate was found to be 167 cm³/s (10 L/min) for both tubes.

The pipe on the detector side of the extinction meter was made longer than the entrance tube, 20 cm vs 15 cm, to reduce the amount of forward-scattered light reaching the detector. The total distance from the centre of the duct to the aperture in the detector assembly is 50 cm, the diameter of the aperture is 1.9 cm, and together they define an acceptance angle of the detector of 1.1°. This value is within the limits set in the report by Putorti.⁹ The forward-scattered light is expected to affect the transmitted intensity by less than 3% even for large soot agglomerates, which scatter strongly in the forward direction. Calculations²⁰ for fractal agglomerates with up to 10⁶ primary spheres with 30 nm diameters, which corresponds to overall cluster sizes up to about 70 µm, are 10% or less scattering in the forward direction for scattering angles less than 1°. Since 70% to 80% of the light-extinction by soot agglomerates²¹ is a result of light absorption, the overall effect of the forward-scattered light on the light-extinction measurement is 3% or less for these agglomerates.

Most of the remaining components of the smoke concentration meter are commercially available. The intention was to provide a design that could be easily duplicated by other laboratories. Of all the smoke concentration meters accepted by the various standard organizations listed in the previous section, our design is closest to ASTM 1354-92. As in the earlier instrument, we also use a He-Ne laser and a silicon detector. Our design uses a laser stabilizer to maintain a constant intensity output with a drift of about 0.1% over a 20 min period. This avoids the custom design of a beam splitter/reference detector assembly as is used in the ASTM Test Method. The stabilizer splits off a small fraction of the beam, monitors the intensity with a Si detector, and adjusts the polarization direction of the liquid crystal polarizer at 4000 Hz to maintain constant intensity. Our original design was based on an electronically stabilized diode laser. This design had the advantage of not requiring an external laser stabilizer. Unfortunately, the temperature controller for the diode assembly was not able to maintain a constant temperature at the required tolerance as the air temperature in the vicinity of the laser increased by several degrees Celsius during a fire test.

The silicon detector was a low-noise detector with a small temperature coefficient and a uniform response over its 1 cm × 1 cm area. A linear amplifier was used rather than the logarithmic amplifier used in the ASTM design. The nominal 2.5 mW He-Ne laser produces a detector signal of about 6 V. The detector has a sensitivity of about 0.3 A/W and is used with a 10 kΩ feedback resistor for the amplifier. The RC time constant for the output with a 10 µF capacitor is 0.1 s. The electronic components were selected to have low temperature coefficients. In addition, all the components were attached to a printed circuit-board within an aluminium housing to minimize temperature change.

The optical assembly included a 1.9 cm aperture, a focusing lens with a 50 mm focal length, and a diffuser

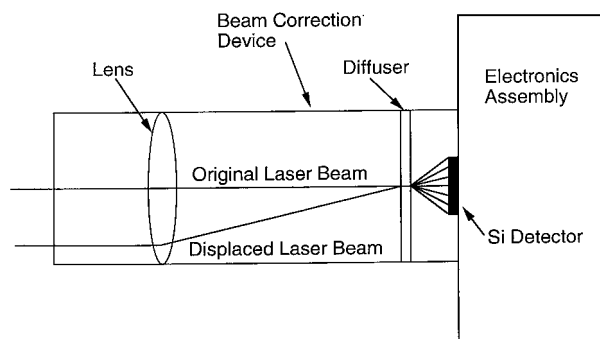


Figure 3. Detection optics.

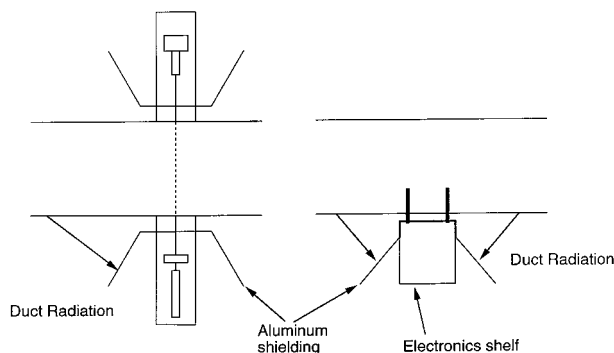


Figure 4. Schematic showing placement of radiation shields.

located near the focus of the lens. Figure 3 illustrates that a parallel displacement of the laser beam will not affect the location of the focal point. The distance to the diffuser was adjusted so that the beam is slightly defocused to avoid a pattern with large speckles resulting from focusing the laser beam on the diffuser. The performance of this assembly in compensating for the effect of slight beam displacements will be discussed in the next section. The combined optics and electronics assembly was designed and fabricated by Reyer Corporation (11847-B Lime Plant Rd., New Market, MD21774).

Other components include mounts for the laser, stabilizer and detector assembly. They are all commercially available except for the laser/stabilizer mounting plate. The following describes the alignment procedure. The laser is first mounted in an adjustable laser holder, which is attached to a plate along with the laser stabilizer. The laser is positioned so that the polarization direction is vertical. The height of the stabilizer and the direction of the laser are adjusted so that the beam passes through the centre of the stabilizer. The plate holding these two components is attached to an x-z positioning stage. Using these adjustments plus shimming of the plate, the laser beam is directed through the centres of both purge tubes. The final step is to position the detector assembly so that the laser beam passes down the centre axis of the optical tube. This process is straightforward because the detector mount assembly includes x-z positioning stages together with tilt control about two axes. The electronic assembly is removed during the alignment process and a target tube is inserted into the optical tube. The positioning equipment was selected both for ease of use and

stability. The alignment process is also simplified because of the relatively large diameter of the optical components and the detector (1 cm) relative to the 2 mm beam diameter of the laser. The electronics package is reinstalled and the detector position is fine tuned to maximize the signal.

One additional component that was not obtained from a commercial source was the radiation shields. These were designed to minimize the radiant heating of the light source, the detector, and the electronics, by thermal radiation from the hot duct. The shields were fabricated of light-weight aluminium and were positioned as indicated in Fig. 4.

EXPERIMENTAL PLAN

The experimental plan was designed to assess the performance of the new smoke concentration meter versus the design specifications given by Putorti⁹ and to assess the uncertainty in measurements of smoke concentration, smoke yield and smoke production rate.

One key measurement regarding the design specification is the drift in the output signal as a function of time for ambient air and hot gases without smoke. Natural-gas fires were used to generate a high-temperature gas flow without smoke. This condition is important for assessing the effect of thermal expansion of the duct on the smoke concentration meter performance. A second key measurement is the light transmitted through selected neutral density filters to assess the linearity of the detector over the range corresponding to light smoke to dense smoke.

To assess the repeatability of the measurement method, the light-extinction coefficient and the smoke yield were measured for propane fires of nominal sizes of 50 kW, 200 kW and 450 kW. At least three repeat measurements were performed on separate days for each fire size. The propane experiments were carried out using a 30 cm square, porous sand burner. Four 6 m³ (220 ft³) propane cylinders were banked together to provide an adequate steady-state flow for fire sizes up to 450 kW. The fuel flow rate was monitored using a diaphragm test meter with a 10 L displacement volume together with a ball flow meter. The pressure within the test meter was monitored with an electronic pressure gauge.

The burner was positioned under the furniture calorimeter's 3.4 m × 3.2 m rectangular hood. The elevation of the hood was 3.5 m and the sides were open up to a height of 1.4 m. The burner top was 0.3 m off the ground. While performing a test, a deflector screen 1.8 m high by 2.5 m wide was positioned about 2.5 m from the hood in the direction of an opened side door to decrease cross flows and keep the plume nominally vertical.

The smoke yield was measured for heptane burning in a 50 cm diameter pan with a 15 cm depth. This was done to allow comparison with previous measurements² of the smoke yield for heptane burning in the same diameter pan. A 1.5 cm layer of fuel weighting about 3 kg was floated on water and a lip height of 1 cm was maintained between the fuel surface and the top of the pan. The burning rate of the fuel was determined using a load-cell

(Mettler-Toledo KB603) with a maximum capacity of 50 kg and a resolution of 1 g. A 2.5 cm thick calcium silicate board (Marinite I) was positioned between the burner and the load cell to minimize the heat transfer between the flame and load cell.

The final experiments consisted of measuring the smoke yield for toluene and toluene–heptane mixtures burning in a 50 cm diameter pan. These experiments tested the smoke concentration meter for high smoke producing fuels approximating the maximum expected for fire testing in the furniture calorimeter.

The determination of the smoke yield required additional instrumentation including a bidirectional probe²² to measure the centreline velocity and a thermocouple to measure the gas temperature. Both of these devices were positioned just downstream of the smoke concentration meter. Additional support measurements include oxygen concentration for determination of heat release rate by oxygen consumption calorimetry¹⁹ and temperature measurements of the wall near the smoke concentration meter and of the gas as it enters the duct above the hood. These data were acquired every 2 s along with the smoke concentration meter data using a scanner box, which multiplexes 60 channels to a 20 bit resolution voltmeter. An AT based computer receives the digitized signal from the voltmeter.

RESULTS

The requirement that the transmitted intensity drift no more than $\pm 0.25\%$ over a 20 min period was readily accomplished with the stabilized He-Ne laser. The typical drift over this period was found to be $\pm 0.1\%$. As discussed in the previous section, the more critical issue is the drift in the beam intensity as the duct is heated by high-temperature gas. The transmitted light intensity was monitored during a 180 kW natural-gas fire. In Fig. 5 the results are expressed in terms of the light-extinction coef-

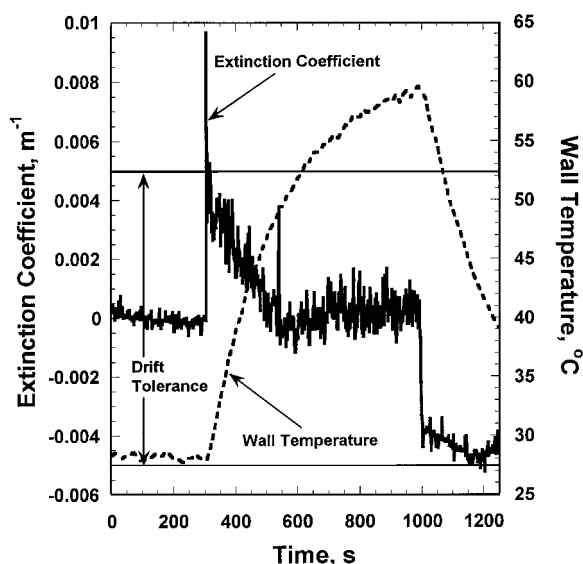


Figure 5. Light-extinction coefficient and wall temperature for 180 kW natural-gas fire.

ficient, K , which is defined by Eqn (2) above, versus time. In computing K , $\ln(I_0)$ is computed as an average over the first 2 min of the test. As seen from Fig. 5, even with the fire present, the extinction coefficient stays within the required drift limits of ± 0.005 for K , which is equivalent to the $\pm 0.1\%$ limits for the intensity. During the experiment the wall temperature increased to about 60°C as the centreline gas temperature increased to about 130°C . The initial increase in K may have been a result of a very low level of smoke being produced from the natural-gas. The increase in the noise during the burning was likely a result of the turbulent fluctuations in the smoke concentration. The change in the background signal to -0.004 resulted from a slight shift in the optical alignment during the heating.

An estimate of the laser beam movement during a fire test was made by observing the beam position both at the detector location and on the wall of the test facility about 7 m from the smoke concentration meter. The test fire was 500 kW which is the maximum fire size for a steady fire in the furniture calorimeter. The beam movement was observed by placing a paper target at the detector location. The measurement resolution for the nominal 3 mm spot size was about 0.5 mm. No beam movement could be detected at this resolution. The beam movement on the wall of the test facility was about 8 mm. Assuming that the displacement on the wall is a result of a slight angular movement of the laser, the computed displacement at the detector position is 1.1 mm, which should be detectable. The fact that no displacement was recorded at the detector location suggests that both the laser beam and detector were displaced at least partially in concert.

A series of measurements were performed with the fire on and off, and slight adjustments were made in the detector position using the vernier adjustments to minimize the drift for the 500 kW fire size. As the duct cools down, the optical assembly returns to its initial alignment as indicated by the decrease in the extinction coefficient. Typically the transmitted beam intensity changes by no more than 0.3% from test to test. There is at least a 10 minute delay between tests to allow for the duct and the bearings in the exhaust blower assembly to cool off.

The second test was to evaluate the linearity of the detector using neutral density filters corresponding to extinction coefficients of 4.74 (10% transmission) and 9.59 (1% transmission). These filters were positioned in a holder mounted to the detector assembly just before the collection optics. The measured values of the extinction coefficient were within 2% of the predicted value. The specification given by Putorti⁵ for the transmitted intensity to be between 2.26% and 2.74% for a 2.5% transmittance corresponds to a range in K of $\pm 2.6\%$. It is suspected that the major cause of the difference between the filter specification and the measured value was not the detector linearity but the accuracy/variability of the neutral density filter. It was noted that the extinction coefficient changed of the order of 2% as the filter was moved.

A measurement was also made with the laser beam turned off. The detector output decreased by a factor of 20000 relative to the incident beam intensity indicating that the smoke concentration meter could be used for

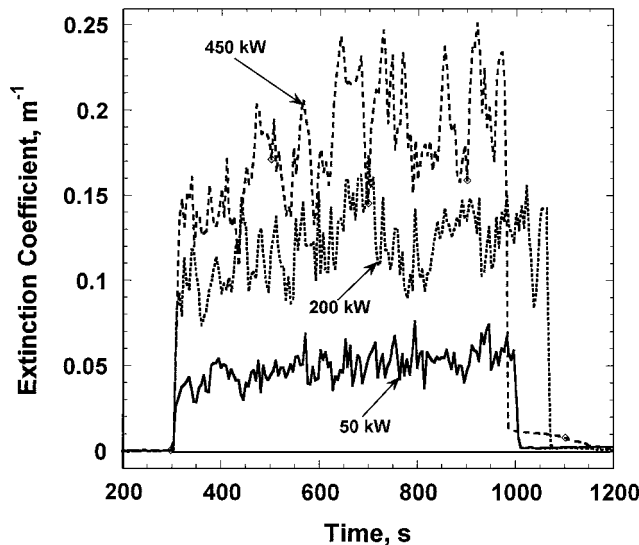


Figure 6. Light-extinction coefficient versus time for propane fires.

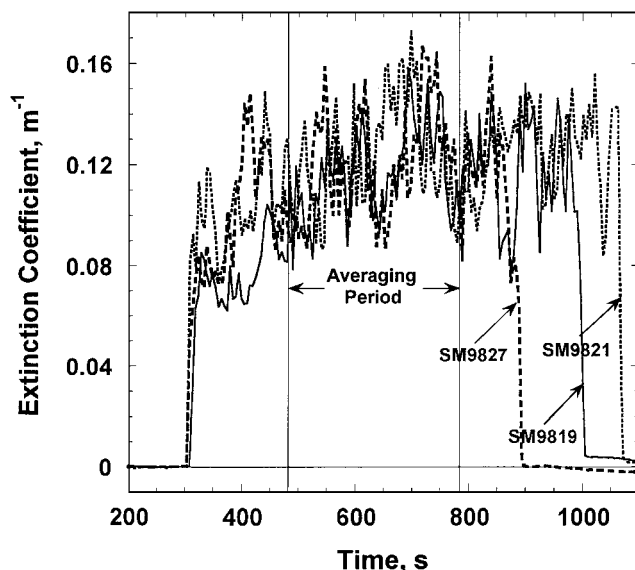


Figure 7. Light-extinction coefficient versus time for triplicate 250 kW propane fires.

transmitted light intensities as low as 0.1% of the incident intensity.

Typically, 5 min of background data were collected at the beginning of each test followed by 10 minutes of burning and another 5 min at the end to verify that the light-extinction returned to its initial value. The extinction coefficient is plotted versus time for tests carried out at nominal heat release rates of 50 kW, 200 kW and 450 kW in Fig. 6. As indicated in this figure, the fluctuation in the light-extinction coefficient is large with a ratio of the standard deviation of the extinction coefficient to the mean value in the range of 0.1 to 0.2. Some fluctuations persist for periods as long as 70 s. An averaging time of 300 s is used for comparing the smoke parameters for the repeat tests. The results from triplicate tests on three separate days for 200 kW propane fires

shown in Fig. 7 suggest that the extinction coefficient on the average is similar for the different tests.

DATA ANALYSIS

There are three types of information that can be obtained from the light-extinction measurements. These are the mass concentration of smoke M_s , the smoke generation rate \dot{m}_s , and the smoke yield ε . By rearranging Eqn (3), M_s can be expressed in terms of the extinction coefficient as

$$M_s = K/\sigma_s \quad (4)$$

To determine the mass generation rate of soot, the mass concentration is multiplied by the volumetric flow rate \dot{V} through the stack and a smoke profile factor C_s , to correct for the slight radial decrease in the smoke concentration near the wall.

$$\dot{m}_s = M_s \dot{V} C_s \quad (5)$$

The volumetric flow rate is computed from the centreline velocity v_c measured with a bidirectional probe, the cross-sectional area of the duct ($A = 0.1847 \text{ m}^2$), and the flow coefficient C_f to correct the centreline velocity to the cross section averaged velocity.

$$\dot{V} = A v_c C_f \quad (6)$$

The coefficients are taken to be 0.83 (C_f) and 0.97 (C_s). The rationales for these choices are given in the uncertainty analysis section. The final quantity of interest is the smoke yield ε , which is defined as the mass production of smoke over a given time interval divided by the amount of fuel consumed over that same time period.

$$\varepsilon = \frac{\sum \dot{m}_{si} \Delta t}{\sum \dot{m}_{fi} \Delta t} = \frac{C_s C_f A \Delta t \sum K_i v_{ci}}{\sigma_s \Delta t \sum \dot{m}_{fi}} \quad (7)$$

The expression on the right hand side of Eqn (7) is obtained in terms of the measured quantities K , v_c , and \dot{m}_f by using Eqn (4–6). Every 2 s the transmitted intensity I and the bidirectional velocity probe data are recorded. The index i is for the i th time step with $i = 1$ corresponding to the start of the averaging period. The quantity K_i is computed using the following modified version of Eqn (2):

$$K_i = \{\ln I_i - \langle \ln I_o \rangle_{avg}\} / L \quad (8)$$

where $\langle \ln I_o \rangle_{avg}$ is the 2 min average before the start of the test. The product of the time increment and the fuel flow rate sum is simply the steady mass flow rate times the averaging time for the case of propane.

The results of the propane tests along with liquid fuel tests are summarized in Table 2. The coefficient of variation (CV), which is defined as the standard deviation divided by the average value, is a metric for measurement repeatability. It is seen that CV for the smoke yield varies from 0.01 to 0.11. The relatively large value of 0.11 for the 50 kW fire arises from the increased uncertainty from the small value of the light-extinction coefficient. It is also possible that for the smallest fires the smoke production is more sensitive to the details of the flow environment in

Table 2. Smoke results from fire tests

Fuel	Nominal heat release rate (kW)	Mass flow of fuel, (g/s)	Mass concentration of smoke, (g/m ³)	Mass flow of smoke (g/s)	Smoke yield	CV ^a for yield
Propane	50	1.07	0.0060	0.0113	0.0106	0.11
	200	4.38	0.0138	0.0278	0.0063	0.01
	450	9.94	0.0248	0.051	0.0052	0.07
Heptane	300	8.90	0.057	0.114	0.0129	0.02
Toluene	250	9.03	0.457	0.903	0.100	
Heptane/Toluene ^b	320	10.63	0.414	0.874	0.082	

^a CV is the coefficient of variation (σ/avg) for the smoke yield.

^b An equal volume mixture of heptane and toluene.

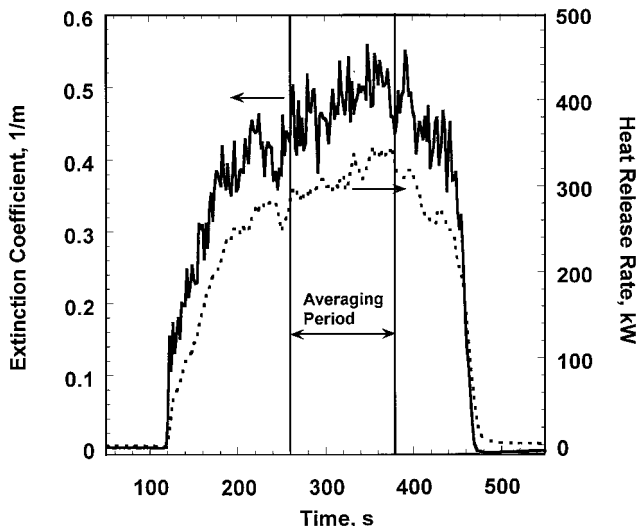


Figure 8. Light-extinction coefficient and heat release rate for a 50 cm diameter heptane pool fire.

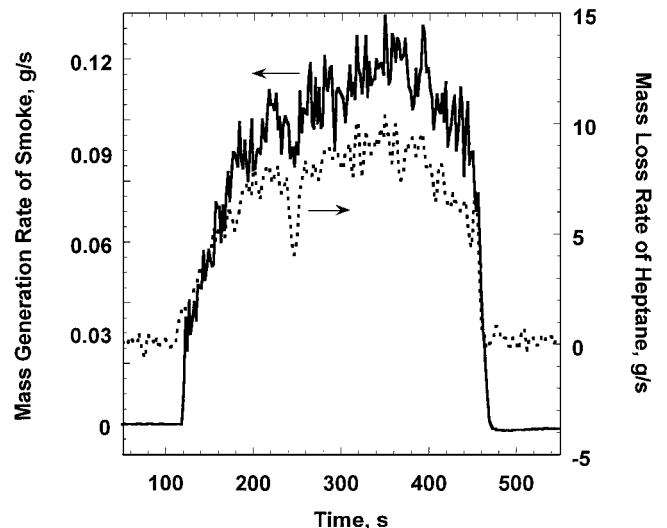


Figure 9. Mass generation rate of smoke and mass loss rate of fuel for 50 cm diameter heptane pool fire. (same test as plotted in Fig. 9)

the fire test room. It is noteworthy that the smoke yield is dependent on the fire scale with about a factor of two decrease in yield as the fire size increases from 50 kW to 450 kW. Sivathanu and Faeth²³ also reported that the smoke yield was sensitive to the fuel flow rate in their experiments with a 5 cm diameter propane burner.

The results from burning 3.5 L of heptane floating on water in a 50 cm diameter pan are plotted in Fig. 8 for the light-extinction coefficient and the heat release rate. The extinction coefficient increases rapidly with time over the first 100 s of burning and then becomes more steady. The fluctuations are similar in magnitude to those observed for the propane flames. It is seen in Fig. 8 that the heat release rate trends are similar to those observed for the extinction coefficient, but the changes are less abrupt resulting from the longer time response required by the oxygen consumption calorimeter.

As discussed above, a load-cell was used to measure the mass loss rate of the liquid fuels. The load-cell data (Mettler-Toledo KB603) are collected every 2 s and a five-point running average is employed to compute the instantaneous mass. As indicated in Fig. 9, the mass generation rate of the smoke follows the same general trend as the mass loss rate of the heptane. The ratio of these two quantities is the instantaneous smoke yield.

The total mass of fuel burned over the 120 s period is computed as the difference between the initial instantaneous mass and the value at the end of the 120 s interval. This value is inserted in the denominator of Eqn. (7) in computing the 2 min averaged smoke yield. As indicated in Table 2, the smoke concentration and smoke yield for heptane are about a factor of 2.5 times larger than those of the largest propane burn. The repeatability of the heptane tests is excellent with a coefficient of variation of 0.02.

To evaluate the operation of the smoke concentration meter for a high soot producer, tests were performed with both toluene by itself and a mixture of toluene and heptane. For the toluene experiment, 3 L were burned in the same 50 cm diameter pool. As indicated in Fig. 10, the light-extinction coefficient reaches a maximum value of 4.4, which is about a factor of 9 larger than for the maximum average value for heptane, and corresponds to about a factor of 9 attenuation in the laser beam intensity. The smoke yield in this case is among the highest measured for hydrocarbon fuels with a value of 0.100 g smoke/g fuel consumed. The smoke concentration meter together with the load-cell performed well for this very smoky flame. Results are also presented in Table 2 for a mixture of 1.75 L toluene and 1.75 L of heptane with the

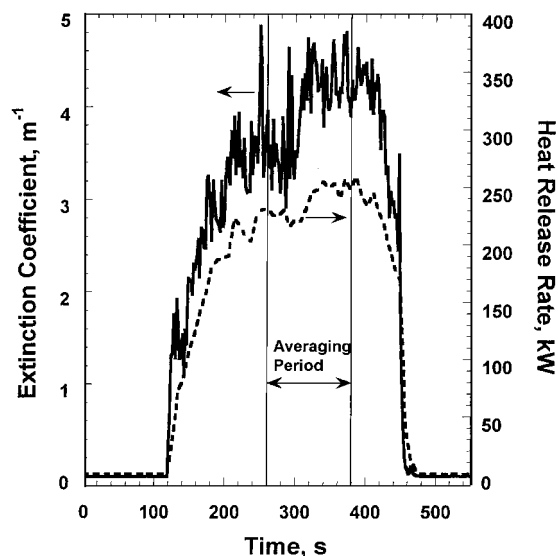


Figure 10. Light-extinction coefficient and heat release rate for a 50 cm diameter toluene pool fire.

yield being much closer to the value obtained for pure toluene. There is no evidence of fractional distillation in the data. Toluene boils at 110°C and heptane at 98°C.

UNCERTAINTY ANALYSIS

The uncertainty analysis presented below provides an overall assessment of the 95% confidence interval for the measurement of smoke yield and smoke production. A uniform methodology for reporting measurement uncertainty has been adopted at NIST,²⁴ which is based on recommendations by the International Organization for Standardization.²⁵ Our uncertainty analysis is based on this recommended method. The components of uncertainty are divided into two categories: Type A are those evaluated by statistical methods and Type B are those evaluated by other means. For the smoke yield measurements the Type A uncertainty is determined by the measurement repeatability while the Type B uncertainty is affected by all the quantities needed for measuring the smoke yield including the light-extinction coefficient, the flow rate, and the burning rate of the fuel. The following section treats these two types of uncertainty separately.

Type A uncertainty

Type A uncertainty is concerned with measurement repeatability. As indicated in Table 2, the coefficient of variation for repeat measurements ranges from 2% to 11%. The average of the four values is 5.3%, which is a measure of the relative standard uncertainty for a single measurement. This represents an average for two fuel types and three fire sizes. The Type A uncertainty for most fuels is expected to be equal or smaller than 5.3%; the exceptions are fuels with small smoke yields of 1% or less burning with a heat release of 50 kW or less.

Type B uncertainty

There are five uncertainty components that affect the smoke yield: the extinction coefficient, the specific extinction coefficient, the volumetric flow rate including the flow coefficient C_f , the smoke profile factor C_s , and the fuel flow rate. Each of these components is affected by more than one subcomponent as discussed below. The uncertainty associated with each of these components is determined and then the effect on the yield is assessed by propagating the uncertainty using the following version of Eqn (7)

$$\varepsilon = \frac{C_s K \dot{V}}{\sigma_s \dot{m}_f} \quad (9)$$

Extinction coefficient K

From Eqn (2) it is seen that the extinction coefficient is affected by the uncertainty in the pathlength and the measurement of the ratio I_o/I . The pathlength through the smoke is determined by visually observing the smoke location as the volumetric flow of purge air is adjusted to just keep the smoke out of the purge tubes. The estimated standard uncertainty associated with the pathlength is 6 mm, which corresponds to a relative standard uncertainty, SD_L , of 1.2%. The nominal drift in the $\ln(I_o/I)$ at a moderate smoke concentration with $\ln(I_o/I)$ equal 0.24 corresponds to a standard uncertainty of 0.0024. This corresponds to a relative standard uncertainty $SD_{\ln I}$, of 1.0%. Using the law of propagation of uncertainties appropriate for relative uncertainties, one finds that the relative standard uncertainty in the extinction coefficient, SD_K , is given by

$$SD_K = \left\{ \left(\frac{\partial \ln K}{\partial L} \Delta L \right)^2 + \left(\frac{\partial \ln K}{\partial \ln(I_o/I)} \Delta(\ln(I_o/I)) \right)^2 \right\}^{1/2} \\ = \{ (SD_L)^2 + (SD_{\ln I})^2 \}^{1/2} \quad (10)$$

where Δ represents the standard uncertainty of the indicated quantities. The resulting value is $SD_K = 1.6\%$. For very low values of the $\ln(I_o/I)$, the drift in the laser intensity can be the largest source of uncertainty. For example, the values of SD_K corresponding to $\ln(I_o/I)$ for the 50 kW propane flame, 0.024, and twice this value, 0.04, are equal 10% and 5%, respectively.

Specific extinction coefficient. From Mulholland and Croarkin⁷ one finds that the recommended value and standard uncertainty for the specific extinction coefficient of flame generated smoke are 8.71 m²/g and 0.47 m²/g. This leads to a relative standard uncertainty equal 5.4%. This is one of the two largest uncertainty components in the analysis. If one is studying a single fuel and has more accurate information on σ_s for this fuel, then this uncertainty component would be reduced.

Volumetric flow rate. The assessment in the uncertainty in the volumetric flow rate is the most involved and is the largest source in the overall uncertainty. One of the sources of uncertainty is the velocity measurement. The velocity is measured by bidirectional velocity probes positioned at the centreline of the duct. McCaffrey and Heskestad²² have calibrated such a probe for Reynolds

number over the range from 40 to 3800 and obtained the following relationship between air velocity, v , and pressure difference, Δp , for large Reynolds numbers.

$$v = \frac{1}{1.08} \left(\frac{2\Delta p}{\rho} \right)^{1/2} \quad (11)$$

From the authors' presentation of their calibration number, the estimated uncertainty in obtaining the velocity from the above equation for Reynolds number greater than 2000 is 3.0% of the velocity reading. Other uncertainties affecting the determination of the velocity include the differential pressure measurement (1%) and the pressure/temperature measurement (each 0.5%), both of which affect the value of the density. Including all these affects, the overall relative standard uncertainty in the velocity measurement is 3.2%.

A second source of flow uncertainty is the relationship between the centreline velocity and the total flow through the duct assuming a radially symmetric flow. The flow coefficient, C_f , is defined through the following equation for the flow \dot{V} through the duct with radius, r_d :

$$\dot{V} = 2\pi \int_0^{r_d} v(r) dr = C_f A v_c \quad (12)$$

where v_c is the centreline velocity. For fully developed turbulent pipe flow, the velocity profile is well fitted to a power law expression such as²⁶

$$v(r) = v_c (1 - r/r_c)^p \quad (13)$$

Substituting v from Eqn (13) into Eqn (12) and solving for C_f , we obtain

$$C_f = 2 \int_0^1 (1 - r^*)^p r^* dr^* \quad (14)$$

The quantity r^* is equal to r/r_d . The integral can be computed analytically with the result,

$$C_f = \frac{2}{(p+1)(p+2)} \quad (15)$$

Schlichting²⁷ has correlated results from several studies on the effect of Reynolds number on the power law. The widely used value of $p = 1/7$ provides a good fit to the velocity profile data at a Reynolds number of 1×10^5 and a corresponding value of C_f equals 0.82. For our experiments the nominal Reynolds number for a flow of 13.5 m/s at a temperature of 100°C is 3×10^5 and the estimated value of p based on interpolating the values given by Schlichting is 1/7.5, which corresponds to C_f equal 0.83. There is no discussion by Schlichting on the uncertainty associated with the power-law expression. From the correlations presented and discussions with Mattingly (personal communication), the estimated standard uncertainty is 0.02. However, this assessment is based on well developed, isothermal turbulent flow; while in the fire experiments, the flow is not isothermal and is not fully developed. There is also the possibility of buoyancy induced flow structures developing in the horizontal flow. To account for these factors the uncertainty in C_f is doubled to 0.04, though it is admitted that this is a rough estimate. Thus, the value of C_f used in our analysis is 0.83 with a relative standard uncertainty of 4.8%.

The one other source of uncertainty is the area of the duct. The duct is fabricated by rolling steel sheets with

1.52 m (5 ft) widths into cylinders and then welding the seam. We estimate the relative standard uncertainty in the duct area as 1.0% based on the variability in the width of the sheets and in the thickness of the butt weld and on the effect of thermal expansion.

Combining these uncertainties as a root-sum-of-squares, we obtain an overall relative standard uncertainty for the volumetric flow rate of 5.9%.

Smoke profile factor. The light-extinction coefficient is a line of sight average, while the mass flow of smoke through the duct is a cross section average weighted by the velocity profile. Assuming that the smoke profile has a form similar to Eqn (13) with centreline concentration M_{sc} and power law p_1 , one obtains the following expressions for the line of sight average \bar{M}_{s1} and the cross section average \bar{M}_{s2}

$$\bar{M}_{s1} = \frac{\int M_s(r) dr}{\int dr} = M_{sc} \frac{1}{(p_1 + 1)} \quad (16)$$

$$\begin{aligned} \bar{M}_{s2} &= \frac{\int 2\pi M_s(r) v(r) dr}{\int 2\pi v(r) dr} \\ &= M_{sc} \left[\frac{\frac{1}{p + p_1 + 1} - \frac{1}{p + p_1 + 2}}{\frac{1}{p + 1} - \frac{1}{p + 2}} \right] \end{aligned} \quad (17)$$

The smoke profile factor, C_s , is the ratio $\bar{M}_{s2}/\bar{M}_{s1}$. If the smoke profile were a constant independent of position, p_1 would equal zero and the two averages would be identical. For the case that both p and p_1 equal 1/7.5, the quantity C_s is equal to 0.95. Smoke concentration profile measurements using a light-scattering-type probe indicate that the smoke profile is flatter than the velocity profile. Based on this finding, we have computed C_s based on a flatter smoke profile with $p_1 = 1/10$ while keeping $p = 1/7.5$ and obtain C_s equal 0.97. We use this as the value of C_s in our data analysis. The estimated relative standard uncertainty is taken as 3% so that the 1 sigma uncertainty range includes the value of C_s equal 1.0, which could happen if the profile is flat or if the peak in the profile is off the centreline.

Fuel flow rate. The estimated uncertainty in the mass flow rate of the propane is 2.2%. A number of factors enter into the determination of the mass flow rate including a nominal 1% relative standard uncertainty in the ambient temperature, ambient pressure and the accuracy of the test meter. The relative uncertainties associated with measuring the time for a fixed volume displacement and the pressure difference between ambient and the value within the test meter were each 0.6%. One other issue is the purity of the industrial quality propane, and this uncertainty is estimated as 1.2%. Combining these effects by the root-sum-of squares, we estimate an overall fuel flow relative standard uncertainty as 2.2%.

The mass-loss measurements for the liquid fuels involve the combustion of about 1 kg over a 120 s period. The reproducibility, 0.55 g, and linearity, 2.5 g, of the load-cell are a small part of the overall relative standard uncertainty of 2.4%. The major components of the uncertainty are the buoyancy, water evaporation, and

measurement noise. To estimate the buoyancy correction, the change in mass of the column of air directly above the load-cell is computed. We make the estimate for a 300 kW fire. Scaling the temperature field data of McCaffrey,²⁸ One finds that the average excess temperature of the column of air defined by the cross section of the pan up to the upper part of the hood is about 300°C. The reduction in mass by the replacement of this 2.5 m height of ambient air at 298 K with air at 598 K is 290 g. The change in mass resulting from buoyancy is much less for the smoke data because the burning rate is relatively steady for the time period that the smoke data is analysed. The typical 7% change in the burning rate corresponds to about a 20 g change in the mass. This, in turn, corresponds to a 2.0% relative standard uncertainty in the mass burned.

A second component in the uncertainty is the evaporation of the water, which is under the 2 cm layer of fuel. As time progresses the thermal wave will reach the water, and then heat the water. This will cause some evaporation of the water. From the mass loss rate of the load-cell at the end of the burn, when only water is present, we obtain an upperbound estimate of about 0.2 g/s. We take half of this value for the water loss near the middle of the test. This corresponds to a relative standard uncertainty of 1.0%.

While the load-cell noise is of the order of 0.2% for a solid material, we find that for a liquid, even without burning, the noise increases to about 0.8%. Presumably the liquid motion caused by convection currents and slight vibrations are responsible for this noise. Combining all these uncertainties as a root-sum-of-squares, one obtains an overall relative standard uncertainty of 2.4%.

Smoke deposition. The final uncertainty is the effect of smoke deposition on the wall leading to a reduced smoke concentration at the measurement location and consequently a reduced smoke yield. There are no quantitative smoke deposition measurements for our flow configuration; in fact, there are very limited quantitative data in general on smoke deposition. It is known that thermophoresis causes high temperature soot particles to deposit on cooler walls. An order of magnitude estimate of the fraction of soot deposited, η , is given by the following formula

$$\eta = 0.5 \frac{(T_{inlet} - T_{sm})}{T_{inlet}} \quad (18)$$

where T_{inlet} is temperature of the gases in the duct just above the hood and T_{sm} is the temperature at the smoke concentration meter. This expression is consistent with smoke deposition measurements by Mulholland *et al.*² For the 300 kW liquid pool fires, the temperature difference is about 10 K and T_{inlet} is about 400 K. The predicted value of η in this case is 0.013. We do not correct for this small change in our smoke yield estimate but do include this factor in our uncertainty analysis as a 1.3% relative standard uncertainty.

Computation of expanded uncertainty. The total Type B uncertainty is computed as the root-sum-of-squares of the individual standard deviations listed in the far right column of Table 3 with the result $\sigma_B = 9.0$. The total Type A and Type B standard uncertainties are combined as

a root-sum-of-squares to obtain the combined relative standard uncertainty of the smoke yield, $u(\varepsilon)$ equal 10.4%. We wish to compute the expanded uncertainty, $U(\varepsilon)$, defined such that there is a 95% level of confidence that the true smoke yield is within $\pm U(\varepsilon)$ of the measured yield. We approximate the relative expanded uncertainty as twice the relative combined uncertainty, $U(\varepsilon) = 2u(\varepsilon)$, with the results $U(\varepsilon)$ equal 20.8%. This is the uncertainty corresponding to a nominal value of the light extinction coefficient equal to 0.5 m^{-1} .

As discussed under the topic 'Specific Extinction Coefficient', as the value of $\ln(I_o/I)$ decreases or, equivalently, K decreases, the uncertainty associated with K increases. The impact of this increase on the total uncertainty will be small until the value of SD_k becomes as large as the largest single component of the uncertainty analysis, the flow uncertainty, with a value 5.9%. For $SD_k = 0.05$, the relative expanded uncertainty is 22.2% compared with 20.8% for $SD_k = 0.016$. For the extreme case of the 50 kW propane flame, the value of K is 0.05, the relative standard uncertainty in K is 10%, which is a factor of 1.7 larger than the flow uncertainty. In this case the relative expanded uncertainty is 28.4%, which is substantially larger than the nominal value of 20.8%. Thus, to obtain a quantitative estimate of the uncertainty in the case of low smoke production, one should compute the uncertainty in K using Eqn (10) and then compute the expanded uncertainty by combining the various sources of uncertainty as done in Table 3.

COMPARISON WITH LITERATURE RESULTS

The heptane tests were performed to allow comparison with literature values of smoke yield for the same size pan and same fuel. The previous study² obtained a value of 0.12 for a 50 cm diameter pan size based on the filter collection of the smoke and subsequent weighing of the soot. There was not a detailed uncertainty assessment in that study; however, the reported standard deviation for repeat experiments was about 10%, and the agreement between the carbon-balance method for measuring smoke yield and the gravimetric method was about 10%. We estimate a relative expanded uncertainty for these measurements of about 20%, which is about the same as the estimate for the smoke concentration meter (20.8%). The difference between the literature value and our result of 0.0129 is 7%, which is about 1/3 of the relative expanded uncertainty. This agreement provides support for the validity of the new smoke concentration meter.

DISCUSSION

We believe our smoke concentration meter design can be utilized by others for incorporation in their fire testing facilities. In Table 1 we have included a list of vendors for the various components. In our case, the smoke concentration meter was mounted on an 0.6 m long section of duct, which was then attached to the existing exhaust duct. The total cost of the components was

Table 3. Uncertainty analysis

Variable	Nominal value	Relative standard uncertainty in variable (%)	Relative standard uncertainty in smoke yield (%)
L	0.485 m	1.2	
$\ln(I_o/I)$	0.24	1.0	
K^a	0.50 m^{-1}	1.6	1.6
σ_s	$8.7 \text{ m}^2/\text{g}$	5.4	5.4
v	13.5 m/s	3.2	
Duct area, A	0.185 m^2	1.0	
Flow coefficient, C_f	0.83	4.8	
Duct flow ^b	$2.1 \text{ m}^3/\text{s}$	5.9	5.9
Smoke profile coefficient, C_s	0.97	3.0	3.0
Fuel flow	10.0 g/s	2.2 (2.4) ^c	2.2
Smoke deposition	0.0	1.2	1.2
Type B relative standard uncertainty			9.0 (7.2) ^d
Type A relative standard uncertainty			5.3
Combined relative standard uncertainty			10.4 (8.9) ^d
Expanded relative standard uncertainty			20.8 (17.8) ^d

^aThe uncertainty in K is computed from the uncertainties in L and in $\ln(I_o/I)$.

^bThe uncertainty in the duct flow is computed from the uncertainties in v , A and C_f .

^cThe value in () corresponds to the uncertainty for the load-cell measurement for liquids with a typical mass loss rate of 8 g/s.

^dExcluding the σ_s component of uncertainty.

approximately \$8000, and another \$2000 was necessary for fabrication of the support structure and optical ports. Such a facility will allow determination of smoke yield and smoke generation rates with little more time or labour than is required for performing heat release rate and mass loss rate measurements.

Possible applications include the real-scale testing of new formulations of fire-retardant chemicals and developing a data base for smoke yield and smoke production rate for commonly occurring materials in constructed facilities. Such data would be useful for modelling of smoke-detector performance, visibility reduction, or radiant heat transfer from a hot smoke layer.

The Cone Calorimeter Apparatus⁶ typically includes a light-extinction measurement, a mass-loss measurement, and a flow measurement so it could be used in the same manner as the smoke concentration meter we have developed. However, before using the instrument for this application, the reliability of the light-extinction measurement should be assessed in terms of the effect of temperature on the beam alignment, the effect of purge flow on the smoke pathlength of about 10 cm, and the repeatability of the measurement method.

The determination of the mass concentration depends on the smoke produced being carbonaceous soot. This is a good approximation for fuels containing only carbon, hydrogen, and oxygen. We have indications that the method also works for nitrogen containing fuels such as polyurethane⁴ and chlorine containing fuel such as polyvinylchloride.⁴ For silicone liquids with silica a major product of combustion, the specific extinction coefficient is much lower than for soot.²⁷

The nature of the combustion will also affect the results. Our analysis applies to overventilated flaming combustion. There are limited data for the case of underventilated burning that suggest the specific extinction coefficient is smaller in this case. We measured σ_s as a function of equivalence ratio using the same apparatus as de-

scribed by Mulholland and Choi²¹ for an underventilated laminar burner³⁰ and found that the value decreased from $8.5 \text{ m}^2/\text{g}$ to $7 \text{ m}^2/\text{g}$ as the equivalence ratio increased from 0.5 to 3.0. So even for rather extreme underventilated burning, the change is modest at 18%. For smouldering or pyrolysis the specific extinction coefficient is lower and much more variable.³¹ The variability results from the smoulder smoke being composed of liquid droplets as opposed to small 'graphitic' soot spherules. The specific extinction coefficient is sensitive to the droplet size distribution and refractive index for the smoulder smoke.

We believe that the uncertainty estimate is a good first order assessment. It includes the first quantitative assessment of the effect of the heating of the duct on the measured light-extinction coefficient. The largest measurement uncertainty is the duct flow with a relative standard uncertainty of 5.9%. There is a need for improved measurements of the duct flow. While the uncertainties associated with the smoke profile and the wall losses were not the largest, the estimates were based on correlations and not on quantitative data.

The uncertainty analysis results summarized in Table 3 are based on a moderate value of the light extinction coefficient K . For small fires with low smoke producing fuels such as the 50 kW propane flame, a quantitative estimate of the expanded uncertainty would be made as described in 'Computation of Expanded Uncertainty' given above.

The smoke yield measurements are based on time averaged samples over a period of 120 s or 300 s. If results are desired over a much shorter time period or if the smoke production changes dramatically over the period of interest, one must account for these effects in the uncertainty analysis. For averaging times of a few seconds, issues to be addressed include the fluctuation in the smoke production from the buoyant flame and the 0.1 s RC time constant of the Si detector output. To

compute the smoke yield requires division by the mass loss rate of the fuel, so one must account for the increased uncertainty in determining mass loss rates from load cell measurements over short time intervals. In our analysis of the load cell data, a 10 s running average (five point) was used.

Acknowledgement

The facility support for the installation of the smoke concentration meter, the data acquisition, the thermocouple and velocity measurements, and the performance of the fire tests was provided by Nelson Brynerk and Gary Roadarmel.

REFERENCES

- Mulholland GW. *The SFPE Handbook of Fire Protection Engineering*, DiNenno PJ, Beyler CL, Custer RLP, et al. (eds) National Fire Protection Association: Quincy, MA 1995; 2-217-227.
- Mulholland GW, Henzel V, Babrauskas V. *The Proceedings of the Second Fire Safety Science International Symposium*, Wakamatsu T, Hasemi Y, Sekizawa A, Seeger PG, Pagni PJ, Grant CE (eds). Hemisphere: New York 1989; 347-357.
- Newman JS, Steciak J. *Comb Flame* 1987; **67**: 55.
- Patterson EM, Duckworth RM, Wyman CM, Powell EA, Gooch JW. *Atm Env* 1991; **25**:2539.
- Wu JS, Krishnan SS, Faeth GM. *J. Heat Transfer* 1997; **119**: 230.
- Babrauskas V. *Development of the Cone Calorimeter - A Bench Scale Heat Release Apparatus based on Oxygen Consumption*, NBSIR 82-2611, National Bureau of Standards Gaithersburg, 1982.
- Mulholland GW. Croarkin accepted for publication in *Fire and Materials*.
- Dobbins RA, Mulholland GW, Bryner NP. *Atm Env* 1994; **28**:889.
- Putorti AD. *Design Parameters for Stack-Mounted Light Extinction Measurement Devices*. NISTIR 99-6215, National Institute of Standards and Technology Gaithersburg, 1999.
- Ohlemiller TJ, Shields JR. *Burning Behavior of Selected Automotive Parts from a Minivan*. NISDTIR 6143, National Institute of Standards and Technology Gaithersburg, 1998.
- ASTM E 84. *Standard Test Method for Surface Burning Characteristics of Building Materials*. American society for Testing and Materials: Philadelphia, 1991.
- ASTM E 662. *Standard Test Method for Specific Optical Density of Smoke Generated by Solid Materials*. American Society for Testing and Materials; Philadelphia, 1997.
- ASTM E 906. *Standard Test Method for Heat and Visible Smoke Release for Materials and Products*. American Society for Testing and Materials; Philadelphia, 1983.
- ASTM E 1354. *Standard Test Method for Heat and Visible Smoke Release Rates for Materials and Products Using an Oxygen Consumption Calorimeter*. American Society for Testing and Materials; Philadelphia, 1992.
- UL 217. *Single and Multiple Station Smoke Alarms*. Underwriters Laboratories Inc.: Northbrook, IL, 1997.
- Myers RL, Aguilar R. *Guidelines for the Use of Commercially Available Transmissometers and Backscatter Devices to Estimate Particulate Mass Loading in Stacks and Ducts*, presented at ASME Joint International Power Generation Conf., Phoenix, AZ, Oct., 1994, available from United Sciences Inc., Gibsonia, PA.
- United States Environmental Protection Agency Method 203. *Determination of the Opacity of Emissions from Stationary Sources by Continuous Opacity Monitoring Systems*. USEPA: Washington, D.C.
- United States Code of Federal Regulations, Vol. 40, Part 60, Appendix B, *Performance Specification 1, Specification and Test Procedures for Opacity Continuous Emission Monitoring Systems in Stationary Sources*. U.S. Government Printing Office.
- ASTM E 1590. *Standard Test Method for Fire Testing of Mattresses*. American Society for Testing and Materials: Philadelphia 1996.
- Mulholland GW, Bryner NP. *Atm Env* 1994; **28**:873.
- Mulholland GW, Choi MY. *27th Symposium (International) on Combustion*, Combustion Institute: Pittsburgh, PA. 1998; 1515-1522.
- McCaffrey BJ, Heskestad G. *Comb, Flame* 1976; **26**: 125.
- Sivathanu YR, Faeth GM. *Comb Flame* 1990; **81**:133
- Taylor BN, Kuyatt CE. *Guidelines for Evaluating and Expressing the Uncertainty of NIST Measurement Results, NIST Technical Note 1297*. National Institute of Standards and Technology: Gaithersburg, 1994.
- Guide to the Expression of Uncertainty in Measurement*, International Organization for Standardization: Geneva. 1993, corrected and reprinted 1995.
- Burmeister LC. *Convective Heat Transfer*. John Wiley and Sons: New York, Chap. 9 1983.
- Shlichting H. *Boundary Layer Theory*. McGraw-Hill: New York. 1968.
- McCaffrey BJ. *Purely Buoyant Diffusion Flames: Some Experimental Results*. NBSIR 79-1910, National Bureau of Standards Gaithersburg, 1979.
- Sivathanu Y, Hamins A, Mulholland GW, Kashiwagi T, Buch R. *7th AIAA/ASME Joint Thermophysics and Heat Transfer Conference*, Vol. 1, 1998; 191.
- Leonard S, Mulholland GW, Puri R, Santoro RJ. *Comb Flame* 1994; **98**: 20.
- Seader JD, Einhorn IN. *16th Symposium (International) On Combustion*. The Combustion Institute: Pittsburgh, 1977; 1423-14 44.